Fibers and Polymers 2018, Vol.19, No.3, 635-640
DOI 10.1007/s12221-018-7755-x

ISSN 1229-9197 (print version)
ISSN 1875-0052 (electronic version)

Evaluating the Mechanical Behavior of Basalt Fibers/Epoxy Composites Containing Surface-modified $CaCO_3$ Nanoparticles

Arezoo Abdi[1], Reza Eslami-Farsani[1]*, and Hamed Khosravi[2]

[1]*Faculty of Materials Science and Engineering, K. N. Toosi University of Technology, Tehran 1999143344, Iran*
[2]*Department of Materials Engineering, Faculty of Engineering, University of Sistan and Baluchestan, Zahedan 9816745845, Iran*

(Received August 29, 2017; Revised November 18, 2017; Accepted November 24, 2017)

Abstract: Polymer matrix composites (PMCs) owing to their outstanding properties such as high strength, low weight, high thermal stability and chemical resistance are broadly utilized in various industries. In the present work, the influence of silanized $CaCO_3$ (S-$CaCO_3$) with 3-aminopropyltrimethoxysilane (3-APTMS) coupling agent at different values (0, 1, 3 and 5 wt.% with respect to the matrix) on the mechanical behavior of basalt fibers (BF)/epoxy composites was examined. BF-reinforced composites were fabricated via hand lay-up technique. Experimental results from three-point bending and tensile tests showed that with the dispersion of 3 wt.% S-$CaCO_3$, flexural strength, flexural modulus, tensile strength and tensile modulus enhanced by 28 %, 35 %, 20 % and 30 %, respectively. Microscopic examinations revealed that the development of the mechanical properties of fibrous composites with the incorporation of modified $CaCO_3$ was related to enhancement in the load transfer between the nanocomposite matrix and BF as well as enhanced mechanical properties of the matrix part.

Keywords: Polymer matrix composites, Basalt fibers, $CaCO_3$ nanoparticles, Surface modification, Mechanical properties, Microscopic examinations

Introduction

From the viewpoint of materials science and engineering, composite materials because of their unique properties like high specific strength and stiffness together with low production costs, are the main choice for employing in aerospace, military and civil applications [1-3]. In the recent years, owing to enhancing demand in environmental issues, natural fibers have gained increasing attention as fibrous reinforcement in composites. Basalt Fibers (BF) as a green industrial material shows various extraordinary properties such as high mechanical strength, desired stability, suitable chemical resistance, and high temperature resistance [4-6]. Since the discovery of basalt as a classified material in 1923 by American scientists, this material had been used during World War II in military research particularly in defense and aerospace applications by America, Europe and the Soviet Union [7]. BF is a favorable selection to replace glass fibers due to their higher mechanical properties, and to carbon fibers due to their significantly less cost. For these reasons, employing BF as a reinforcing phase in composites has attracted much attention and a number of researches have been conducted to determine the mechanical behavior of this type of composites under various loadings [8-10].

In the recent years, improvement in mechanical properties of fibrous composites has gained much attention of researchers. In this regard, adding nanoparticles as a second reinforcing phase to the structure of specimens has been evaluated by several investigators. Generally, nanoparticles can be entered into the structure of composites in two ways. In the first method, nanoparticles directly dispersed into the matrix by applying ultrasonic waves and high speed stirring, while in the second method, they are grown onto the surface of fibers [11-15].

He *et al*. [16] reported that compressive properties of nano-$CaCO_3$/epoxy/carbon fiber composites based on the modified epoxy matrix were enhanced. In Ref. [17] it was reported that the addition of 4 wt.% nano-$CaCO_3$ led to 36.6 % increase in the interlaminar shear strength (ILSS) for the carbon fiber/epoxy composite. Zulfli *et al*. [18] asserted that with the mixing of 8 wt.% nano-$CaCO_3$ within the epoxy matrix, fracture toughness of glass fiber/epoxy composites increased about 12 %. Xia *et al*. [19] showed that the tensile properties of kenaf fiber/polyester composites containing $CaCO_3$ nanoparticles. Their results revealed that tensile strength of $CaCO_3$-enhanced composites was 67.8 % higher than the composite without nanofiller. Mirzapour *et al*. [20] demonstrated that the flexural strength of carbon fiber/phenolic composites improved by 13 % through the dispersion of 3 wt.% nanosilica into the phenolic matrix.

Krushnamurty *et al*. [21] investigated the reinforcing effect of surface modified nanoclay particles on the flexural properties of glass-fiber/epoxy composites. They reported that with the incorporation of 3 wt.% of nanoclay, flexural strength of the fibrous composite increased by 12 %. Anbusagar *et al*. [22] demonstrated that by adding 4 wt.% of nanoclay, flexural strength and modulus of glass fiber/ polyester composites compared with control one increased by 40 and 57 %, respectively; while at higher amounts of nanoclay, flexural properties were decreased due to the agglomeration. Manjunath *et al*. [23] reported that introduction of 3 wt.% of nano-Al_2O_3 particles caused the improvement

*Corresponding author: eslami@kntu.ac.ir

in flexural strength and impact strength of unidirectional glass fiber/epoxy composites about 6 % and 22 %, respectively. Uddin *et al*. [24] studied the effect of SiO_2 nanoparticles on the mechanical response of unidirectional glass fiber/epoxy composites fabricated by vacuum resin transfer molding and indicated the improvement in the tensile and compression strengths of composites.

According to literature, no research work has been carried out in regard to the reinforcing of BF-reinforced polymer matrix composites with $CaCO_3$ nanoparticles. Therefore, the aim of the present study was to demonstrate the role of silane-modified $CaCO_3$ nanoparticles on the mechanical properties of BF/epoxy composites under tensile and three-point bending loadings.

Experimental

Materials

In the present study, KER 828 epoxy resin and polyamine curing agent supplied by Kumho P&B chemicals, Inc., was used as polymer matrix of specimens. BF having a satin texture and surface density of 300 g/m^2, was supplied by Basaltex Co., Belgium. $CaCO_3$ nanoparticles with mean diameter of 50 nm were supplied by US Nanomaterials Co., USA. Sialne coupling agent with commercial name of 3-aminopropyltrimethoxysilane (3-APTMS) from Merk Co., was employed for surface modification of $CaCO_3$ nanoparticles. Various properties of raw materials employed in this research are given in Table 1.

Surface Modification of $CaCO_3$ Nanoparticles

In order to enhancing the interaction of the $CaCO_3$ nanoparticles with epoxy matrix, surface modification of nanoparticles is necessary. In the first stage, 5 g of $CaCO_3$ nanoparticles were mixed in 100 m*l* solution including 95 % ethanol and 5 % water. Then, 3-APTMS with the same weight ratio regarding to $CaCO_3$ was added to the mixture. The obtained mixture was exposed to the ultrasonic waves for 10 min and then reflux treatment was conducted at 80 °C for 8 h. pH of mixture was adjusted in range of 4-5 by using hydrochloric acid [13]. After this stage, for extracting the $CaCO_3$ nanoparticles, the mixture was centrifuged under velocity of 4000 rpm for 30 min. Finally, $CaCO_3$ nanoparticles were washed three times with ethanol to remove the surplus coupling agent on them and then placed in oven at 80 °C for 12 h.

Table 1. Some properties of the raw materials used in this study

Material	Property (unit)	Value
KER-828 epoxy	Combined density (g/cm^3)	1.16
	Viscosity at 25 °C (Pa·s)	12-14
	Vapor pressure at 25 °C (Pa)	0.01
Basalt fibers fabric (BF)	Apparent density (g/m^2)	300
	Thickness (mm)	0.3
$CaCO_3$ nanoparticles	Mean diameter (nm)	50
	Purity (%)	98
	Specific gravity (g/cm^3)	2-3
	Moisture (wt.%)	<0.4

Fabrication of Specimens

S-$CaCO_3$ nanoparticles with various weight contents (0, 1, 3 and 5 wt.%) with respect to the whole weight of the matrix including resin and curing agent were added. Initially, the epoxy/$CaCO_3$ mixture was stirred using a high speed shear mixing (Finetech, Korea) at rotational speed of 2000 rpm for 20 min. Then, the ultrasound waves were exerted into the obtained mixture using a probe sonicator (FAPAN, Iran) with frequency of 24 kHz and power of 120 W for 60 min. In order to remove air bubbles, degasification of the mixture was accomplished under vacuum conditions. Finally, curing agent with a weight ratio of 100:10 was added to the mixture. The resultant mixture was used as matrix for fabricating the fibrous composites. BF/epoxy/S-$CaCO_3$ multiscale specimens were prepared by hand lay-up method, in which 6 layers of BF with volume percentages of ~50 % was employed.

Mechanical Tests

Three-point bending and tensile tests were conducted at room temperature according to ASTM D790-10 and ASTM: D3039-08, respectively. Hounsfield H25KS testing machine was employed to conduct the tests. Loading velocity for tensile and bending tests were 5 and 4.3 mm/min, respectively. For three-point bending test, the distance between supports was 80 mm. At least, three specimens from each condition were examined and the average data was reported.

Characterization

To characterize the functional groups on the $CaCO_3$ surface, Fourier-Transform Infrared (FTIR) spectroscopy spectra of unmodified and modified $CaCO_3$ nanoparticles, a JASCO FTIR spectrometer (FTIR-460 plus) was used. The powders were analyzed at wavenumbers of 400-4000 cm^{-1}, with a sensitivity of 4 cm^{-1}. Microstructures of the composites after mechanical tests were comparatively evaluated using a TESCAN scanning electron microscopy (SEM) under voltage of 25 kV.

Results and Discussion

FTIR Examination

To understand the chemical structure of untreated $CaCO_3$ and S-$CaCO_3$ nanoparticles, they were studied by FTIR spectroscopy and the results are shown in Figure 1. In the case of untreated $CaCO_3$, the observed peak at 3422 cm^{-1} is due to the stretching vibrations of hydroxyl (OH) groups [25,26], while the peaks at 2913 cm^{-1} and 2849 cm^{-1} are

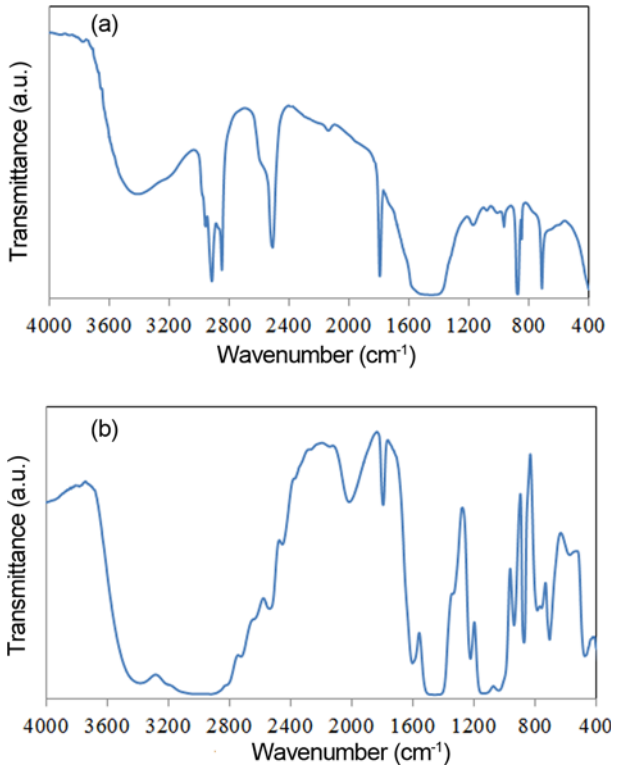

Figure 1. FTIR spectra of (a) untreated $CaCO_3$ and (b) S-$CaCO_3$.

related to the CH_3 asymmetric stretching and CH_2 stretching [27]. Absorptions at 712 cm^{-1}, 880 cm^{-1} and 1470 cm^{-1} are the characteristic bands for carbonate mineral, calcite [28]. Also, the band appearing at 1794 cm^{-1} is due to the C=O group of carbonate ions. The FTIR spectrum of the S-$CaCO_3$ shows additional peaks at 1597 cm^{-1} (corresponded to the bending vibration of N-H groups) [29], 2952 cm^{-1} (assigned to -NH_2) [29], and 1227 cm^{-1} (related to the Si-O group stretching vibration) [29,30] which are absent in the FTIR spectrum of the untreated $CaCO_3$, confirming the successful 3-APTMS grafting to the $CaCO_3$.

Results of Mechanical Tests

The results of tensile and three-point bending tests for multiscale BF/epoxy composites containing different weight percentages of S-$CaCO_3$ nanoparticles are shown in Table 2 and Figures 2-4. The effect of S-$CaCO_3$ addition on the tensile and flexural strengths of composites is given in Figure 2. As can be inferred from this graph, the observed trend for both the tensile and flexural strengths with increasing the S-$CaCO_3$ loading is increasing at the first step and then decreasing. The greatest strength values are regarded to the specimen with 3 wt.% S-$CaCO_3$. For this specimen, 20 % and 28 % increment can be seen in tensile and flexural strengths, respectively compared to the neat BF/epoxy composite. Increasing the strength of fibrous composites arising from the presence of S-$CaCO_3$ nanoparticles is due to the enhancement of the interfacial characteristics between the BF and matrix [31] as well as improving the mechanical properties of the matrix. When the matrix is filled with the nanoparticles, a portion of applied load is tolerated by them. Moreover, in the presence of S-$CaCO_3$ the frictional slippage between the matrix and fibers is impeded via pinning mechanism. Also the addition of S-$CaCO_3$ nanoparticles within the matrix can decrease the stress concentration onto the BF during mechanical loading and as a result increase the required stress for the fiber failure. In the other words, with the dispersion of nanoparticles, a part of the applied load to the composite is carried by the nanoparticles [32]. However, the addition of higher content of S-$CaCO_3$ (i.e. 5 wt.%) causes the reduction in tensile and flexural strengths. Lower strengths of the 5 wt.% S-$CaCO_3$ loaded specimen compared to the specimen containing 3 wt.% S-$CaCO_3$ can be attributed to the decrease of adhesion between the matrix and BF due to the creation of non-continuous network within the matrix and formation of the agglomerates. The agglomerates of nanoparticles within the matrix can act as stress concentration regions, reducing the mechanical properties.

Another result which can be deduced from Figure 2 is that the effect of S-$CaCO_3$ at a specified weight percent on the flexural strength is greater than the tensile strength. Under three-point bending, the specimen above the neutral axis is under compression and below the neutral axis is under tension. In this case, matrix plays a more effective role than tensile testing. According to this fact, through the reinforcing of matrix with S-$CaCO_3$ nanoparticles a higher enhancement in the flexural strength can be obtained.

Effect of S-$CaCO_3$ loading on the tensile and flexural moduli of BF/epoxy composites is shown in Figure 3. As it can be seen, with the addition of 3 wt.% S-$CaCO_3$ tensile and flexural moduli are increased by 30 % and 35 % compared to the specimen without S-$CaCO_3$ addition.

Table 2. Results of the three-point bending and tensile tests of basalt fibers-$CaCO_3$ nanoparticles/epoxy composites

$CaCO_3$ loading (wt.%)	Flexural strength (MPa)	Flexural modulus (GPa)	Tensile strength (MPa)	Tensile modulus (GPa)
0	435.86±13.07	18.56±0.55	414.1±16.56	15.32±0.61
1	479.52±16.78	20.97±0.52	447.55±17.3	16.85±0.71
3	557.90±22.3	25.05±1.02	497.28±24.86	19.91±0.59
5	523.03±18.25	25.98±1.16	476.63±21.44	20.83±0.93

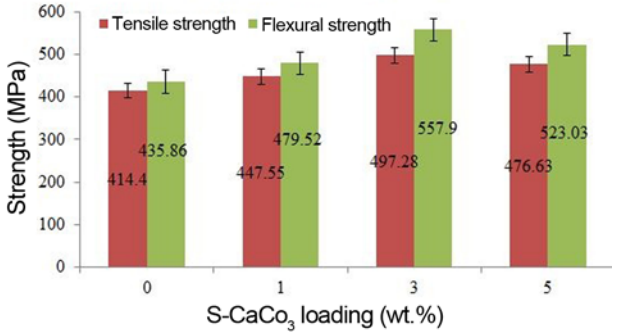

Figure 2. Effect of S-$CaCO_3$ loading on the flexural and tensile strengths of specimens.

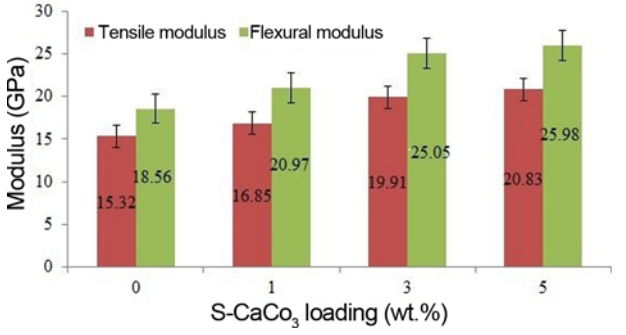

Figure 3. Effect of S-$CaCO_3$ loading on the flexural and tensile moduli of specimens.

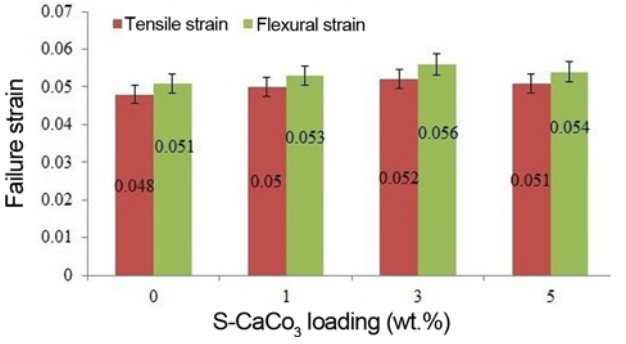

Figure 4. Effect of S-$CaCO_3$ loading on the flexural and tensile failure strains of specimens.

Besides, in the case of 5 wt.% S-$CaCO_3$, tensile and flexural moduli are enhanced by 36 and 40 %, respectively. The observed trend suggests the reduction in the rate of increase in the moduli at higher weight percentages. Dispersion of S-$CaCO_3$ in the matrix restricts the movement of the polymeric chains which consequently enhances the stiffness of the composite. Also, because of the higher stiffness the $CaCO_3$ nanoparticles compared to the epoxy, improvements in the moduli (tensile and flexural) can be expected. Non-uniform dispersion of $CaCO_3$ at higher loading (see later section) reduces the effect of them for improving the modulus of composites.

According to Figure 4, with dispersion of various weight percentages of S-$CaCO_3$ nanoparticles, the failure strains (tensile and flexural) of BF/epoxy composites are firstly increased up to 3 wt.% and then declined. At 3 wt.% S-$CaCO_3$, the tensile and flexural failure strains enhances by 8 and 10 %, respectively. In this regard, deflection of the cracks by nanoparticles within the matrix improves the fracture toughness of composites. When the crack tip reaches to the nanoparticles dispersed in the matrix, they alter the growth direction. In fact, the dispersion of nanoparticles creates strong barriers against the crack propagation, causing the prevention of brittle failure and increasing the failure strain. Similar to the observed trend for strengths, decline in the tensile and flexural failure strains with incorporation of 5 wt.% S-$CaCO_3$ compared to the specimen with 3 wt.% S-$CaCO_3$ can be related to the unfavorable dispersion of nanoparticles which can act as stress concentration regions.

Microscopic Examination

Figure 5 illustrates the fracture surfaces of the composites without and with 3 wt.% S-$CaCO_3$ incorporation. For neat specimen without $CaCO_3$ nanoparticles (Figure 5(a)), the smooth surface of fibers without trace of matrix on them indicates an improper adhesion between epoxy matrix and BF. In contrast, for multiscale specimen containing S-$CaCO_3$ (Figure 5(b)), presence of remained matrix onto the surface of BF demonstrates a good interface between the nano-compoite matrix and BF.

Figure 6 shows the fracture surface morphology of the pure epoxy and epoxy/S-$CaCO_3$ nanocomposite matrix. As

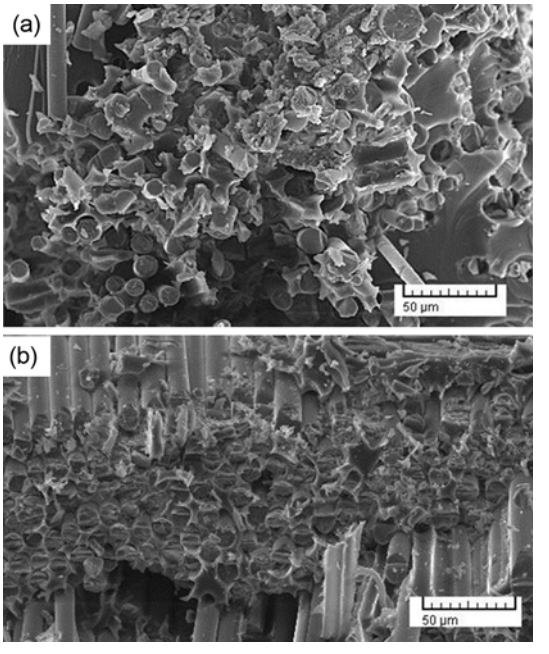

Figure 5. SEM images from fracture surface of specimens (a) without and (b) with 3 wt.% S-$CaCO_3$ addition.

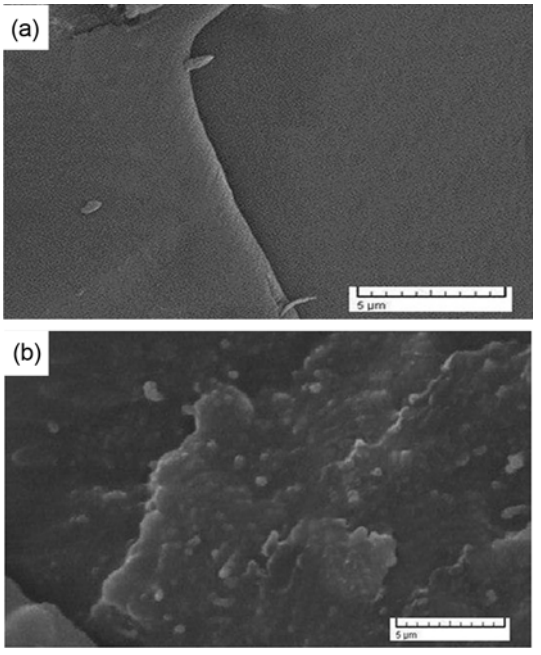

Figure 6. SEM images from the (a) neat matrix and (b) epoxy/ 3 wt.% S-$CaCO_3$ nanocomposite matrix.

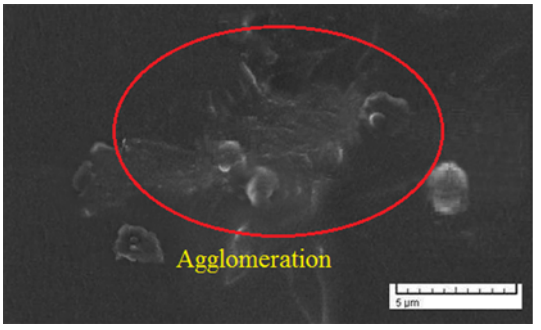

Figure 7. Formation of agglomerates of S-$CaCO_3$ within the matrix of specimen filled with 5 wt.% S-$CaCO_3$.

can be seen from Figure 6(a), the fracture surface of pure epoxy is flat manifesting the brittle failure and propagation of crack in direct path [13,27]. However, in the case of polymeric matrix with 3 wt.% S-$CaCO_3$ nanoparticles (Figure 6(b)), the fracture surface is ragged and the crack deflection mechanism [32] is well observable. It means that S-$CaCO_3$ nanoparticles act as tough barriers against the crack propagation. Figure 7 exhibits the existence of agglomeration in the case of 5 wt.% $CaCO_3$ loaded specimen, which acts as stress concentration regions and in turn degrades the mechanical properties of the composite. So, it can be concluded that the methods used for improving the dispersion of $CaCO_3$ nanoparticles in the matrix was not suitable for high weight percentages of nanoparticles, and other methods should be employed.

Conclusion

In this work, the influence of adding silane-modified $CaCO_3$ (S-$CaCO_3$) nanoparticles on the mechanical properties of basalt fibers/epoxy composites under three-point bending and tensile conditions was experimentally investigated. The obtained results are as follows:

1. FTIR spectroscopy results revealed that the surface modification of $CaCO_3$ nanoparticles with silane coupling agent was successfully accomplished.
2. Mechanical properties of basalt fibers/epoxy composites were enhanced with the addition of S-$CaCO_3$ nanoparticles. The highest improvements were obtained through the addition of 3 wt.% S-$CaCO_3$. For this specimen the flexural strength, flexural modulus, tensile strength and tensile modulus in comparison with control specimen were enhanced by 28 %, 35 %, 20 % and 30 %, respectively.
3. For basalt fibers/epoxy composite reinforced with 5 wt.% S-$CaCO_3$ nanoparticles, the tensile and flexural strengths were decreased compared to the specimen having 3 wt.% S-$CaCO_3$.
4. The results of SEM observations approved that the addition of S-$CaCO_3$ nanoparticles resulted the favorable adhesion between epoxy matrix and basalt fibers which had a notable role in improving the mechanical properties of composites.

References

1. M. R. Sanjay, G. R. Arpitha, and B. Yogesha, *Mater. Today: Proceeding*, **2**, 2959 (2015).
2. P. K. Mallick, Taylor & Francis Group, LLC, 2007.
3. S. Jambari, M. Y. Yahya, M. Ruslan, and A. M. Jawaid, *Fiber. Polym.*, **18**, 563 (2017).
4. G. Wu, X. Wang, Z. Wu, Z. Dong, and G. Zhang, *J. Compos. Mater.*, **49**, 873 (2015).
5. B. Sun, Z. Niu, L. Zhu, and B. Gu, *J. Compos. Mater.*, **44**, 1779 (2010).
6. B. Wei, H. Cao, and S. Song, *Mater. Sci. Eng. A*, **527**, 4708 (2010).
7. J. Militky, V. Kovacic, and J. Rubnerova, *Eng. Fract. Mech.*, **69**, 1025 (2002).
8. J. J. Lee, I. Nam, and H. Kim, *Fiber. Polym.*, **18**, 140 (2017).
9. H. Kim, *Fiber. Polym.*, **14**, 1311 (2013).
10. M. A. Shayed, R. D. Hund, and C. Cherif, *Fiber. Polym.*, **15**, 2086 (2014).
11. M. Karahan and A. Godara, *J. Reinf. Plast. Compos.*, **32**, 515 (2013).
12. C. M. Hadden, D. R. Klimek-McDonald, E. J. Pineda, J. A. King, A. M. Reichanadter, I. Miskioglu, S. Gowtham, and G. M. Odegard, *Carbon*, **95**, 100 (2015).
13. H. Khosravi and R. Eslami-Farsani, *J. Reinf. Plast. Compos.*, **35**, 421 (2016).

14. S. S. Du, F. Li, H. M. Xiao, Y. Q. Li, N. Hu, and S. Y. Fu, *Compos. Pt. B-Eng.*, **99**, 407 (2016).
15. H. Ulus, O. S. Sahin, and A. Avc, *Fiber. Polym.*, **16**, 2627 (2015).
16. H. He, Z. Zhang, J. Wang, and K. Li, *Compos. Pt. B-Eng.*, **45**, 919 (2012).
17. H. He and F. Gao, *Polym. Compos.*, doi:10.1002/pc.23775 (2015).
18. N. H. M. Zulfli, A. AbuBakar, and W. S. Chow, *High Perform. Polym.*, **26**, 223 (2014).
19. C. Xia, S. Q. Shi, and L. Cai, *Compos. Pt. B-Eng*., **78**, 138 (2015).
20. A. Mirzapour, M. H. Asadollahi, S. Baghshaei, and M. Akbari, *Compos. Pt. A-Appl. Sci. Manuf.*, **63**, 159 (2014).
21. K. Krushnamurty, I. Srikanth, B. Rangababu, S. K. Majee, R. Bauri, and C. Subrahmanyam, *Adv. Mater. Lett*., **6**, 684 (2015).
22. N. R. R. Anbusagar, K. Palanikumar, R. Vigneswaran, M. Rajmohan, and P. Sengottuvel, *Appl. Mech. Mater.*, **766**, 372 (2015).
23. M. Manjunath, N. Renukappa, and B. Suresha, *J. Compos. Mater.*, **50**, 1109 (2016).
24. M. F. Uddin and C. T. Sun, *Compos. Sci. Technol.*, **68**, 1637 (2008).
25. M. Mozaffari Naiini, M. Ghahari, and M. Sh. Afarani, *Particul. Sci. Technol*., **33**, 456 (2015).
26. M. Araghi, M. Ghahari, and M. Sh. Afarani, *J. Environ. Chem. Eng.*, **5**, 1780 (2017).
27. H. Khosravi and R. Eslami-Farsani, *Polym. Test.*, **55**, 135 (2016).
28. Z. Yao, M. Xia, L. Ge, T. Chen, H. Li, Y. Ye, and H. Zheng, *Fiber. Polym.*, **15**, 1278 (2014).
29. S. Shan, X. Chen, Z. Xi, X. Yu, X. Qu, and Q. Zhang, *High Perform. Polym.*, **29**, 113 (2017).
30. H. He and F. Gao, *J. Macromol. Sci. B*, **54**, 879 (2015).
31. A. Shahrabi-Farahani and R. Eslami-Farsani, *Fiber. Polym.*, **18**, 965 (2017).
32. H. Khosravi and R. Eslami-Farsani, *J. Comput. Appl. Res. Mech. Eng.*, **7**, 99 (2017).